International Journal of Research in Engineering and Science (IJRES)
ISSN (Online): 2320-9364, ISSN (Print): 2320-9356
www.ijres.org Volume 14 Issue 1 ǁ January 2026 ǁ PP. 19-34

Comparative Numerical Assessment of Flexural Repair against Mid Span Rebars Cut Using either Conventional Steel Rebars or Steel Plate or Carbon Fiber Sheet

Zeinab Hussein[1], Alaa Eldin Y. Aboelezz[1]
[1]*Civil Engineering Department, Faculty of Engineering, Minia University, Minia, Egypt*
Corresponding Author: Zeinab Hussein

Abstract
Repairing and retrofitting has become of importance for reinforced concrete beams. The literature mostly provide singular methods showcasing their effectiveness. This study provides comparative assessment for two conventional and simple repairing methods using finite element analysis models with ANSYS, this is to repair a damage case of reinforcement cut of lower rebars at the mid span of a simple beam. The first method is the application of rebars of the same number and diameter, with various added lengths as percentages of development length. The second method is the application of a planar repair material, here, CFRP sheet and steel plate. Finite element validation is firstly carried out based on another experimental damage case of overall corrosion of reinforcement from the literature, this is in order to fetch the parametric values of concrete material models based on a realistic case, and then the damage case is developed with a certain scale relative to the experimental work. The best repair case for the damage case proof-of-concept models is the one with the use of rebars with full to half the development length, and the least effective repair case is the use of steel plate applied onto the lower soffit of the beam, and the use of CFRP sheet is slightly better than using steel plate but both of them are lower than the first method of using rebars.

Keywords: *Comparative, Repairing, ANSYS, Damage, Cut, Reinforcement, Rebars, CFRP sheet, Steel plate.*

Date of Submission: 27-12-2025 Date of acceptance: 06-01-2026

I. INTRODUCTION

Reinforced concrete beams occasionally undergo damage during service time or even at the construction stage. Mostly, they are designed to withstand flexural effect through spans of loading. Multiple methods were suggested for the repairing and retrofitting of beams such as jacketing or the usage of steel plates, CFRP sheets and rods either applied externally bounded or near surface mounted.

This study focus on comparison between two simple methods of repairing, namely, using conventional steel rebars or using sheets made whether from steel or carbon fiber.

A damage case of cutting lower longitudinal rebars at a segment of the mid span is presented, the removal of the reinforcement which is supposed to withstand flexure opens the way to investigate the effectiveness of these repairing methods.

Moreover, the validation numerical finite element models aiming for setting the parametric values of concrete's material model are based on a case study of experimental work that grasps the effect of reinforcement corrosion onto the degradation of flexural performance. Hence, shedding light onto how strategic simplicity can reach satisfactory sufficient results.

1.1. Literature Review of Recent Relevant Works

Siddika et al. (2019) [1] provide a comprehensive review of the use of fiber-reinforced polymer (FRP) composites for strengthening reinforced concrete beams. The study details various FRP types, such as glass FRP (GFRP) and carbon FRP (CFRP), highlighting their mechanical properties, including tensile strength (400–4000 MPa), elastic modulus (50–600 GPa), and rupture strain (0.5–2.5%). GFRP is noted for its high stiffness and alkali resistance but lower tensile strength compared to CFRP, which is more expensive. The review discusses the influence of material properties, environmental conditions, and cost on FRP selection for structural strengthening, emphasizing GFRP's suitability for specific applications due to its cost-effectiveness and performance.

Habib et al. (2018) [2] conducted a nonlinear finite element analysis using ANSYS to evaluate the behavior of RC beams strengthened with externally bonded CFRP sheets in both flexure and shear. Their models

showed good agreement with experimental results, with improved ultimate capacity due to CFRP strengthening. Parametric studies confirmed that increasing CFRP layers and using continuous U-wraps significantly enhance performance, especially in shear.

Samani et al. (2018) [3] experimentally investigated the torsional strengthening of RC beams using different configurations of externally bonded CFRP laminates. The study demonstrated that CFRP wraps significantly increase the torsional capacity and ductility of beams, with full U-wraps offering superior performance compared to side-bonded laminates. The research also provided failure mode observations and emphasized the influence of wrap configuration on torsional behavior.

Mattar (2019) [4] developed a finite element (FE) modeling procedure using ABAQUS CAE 6.11-3 to simulate the behavior of reinforced concrete (R.C) beams retrofitted with fiber-reinforced polymers (FRP) in bending. The study compared isotropic and orthotropic FRP material models, finding similar results, and evaluated perfect bond and cohesive zone models for the concrete-FRP interface, with the latter capturing debonding. Validated against experimental data, the FE model accurately predicted load-deflection curves and cracking patterns. Parametric studies showed that increasing FRP sheet width enhances stiffness and load capacity at longer lengths, while additional FRP layers increase stiffness but not load capacity, only shifting the yielding point.

Kim and Lee (2021) [5] proposed a modularized steel plate retrofitting method for reinforced concrete (R.C.) beams to enhance structural performance and constructability. Using ANSYS 16.0 for finite element analysis, they optimized L-shaped and Z-shaped steel plates, fixed with chemical anchors and bolts, to reduce weight and improve installation. Five beam specimens (one control, four retrofitted) were tested, showing a 3-fold increase in flexural strength, 2.5-fold increase in ductility, and 7-fold increase in energy dissipation capacity compared to the control. The method minimizes welding, reduces stress concentration, and enhances rapid construction.

Shadmand et al. (2020) [6] investigated retrofitting reinforced concrete (R.C.) beams using steel fiber reinforced concrete (SFRC) jackets, steel-concrete composite jackets, and CFRP sheets. Ten beams were tested, with jackets covering 75% of the beam's peripheral surface. Steel fibers (0%, 1%, 2%) enhanced tensile strength, stiffness, and energy absorption. Composite jackets with 1% steel fibers showed the highest ultimate strength (232% increase in crack load), ductility (300% increase), and energy absorption (377-716% increase) compared to the control. CFRP sheets improved ductility (78%) but had lower energy absorption due to debonding. Steel-concrete composite jackets outperformed others in stiffness (22% increase) and load capacity.

Ghalla et al. (2024) [7] investigated strengthening reinforced concrete (R.C.) beams with insufficient lapped splice lengths using externally bonded CFRP sheets and near-surface mounted (NSM) CFRP bars. Twelve full-scale beams were tested, varying in splice length and strengthening method. Both techniques improved load capacity (up to 60%) and ductility, with NSM CFRP bars outperforming sheets in preventing splice failure and enhancing bond strength. Load-deflection curves validated the effectiveness of both methods.

In summary, the recent trend of research focus tends to a degree of complexity of dealing with this problem, while this is beneficial in the creation of a multiple proposals, however, simplicity mainly dictates the field of construction, hence, the need for a comparative reference between simple approaches, and this is the focal point of this study.

1.2. Numerical Finite Element Validation

The work of numerical validation is based on Nguyen et al. (2019) [8], which examined the flexural behavior of corroded reinforced concrete beams using an electrochemical accelerated corrosion method. Six beams, divided into two groups based on tension reinforcement ratios (D8 and D10 bars), were tested under four-point bending. Figures {1,2,3} illustrate the schematic of the tests, the mechanical properties of rebars, and the corrosion rates.

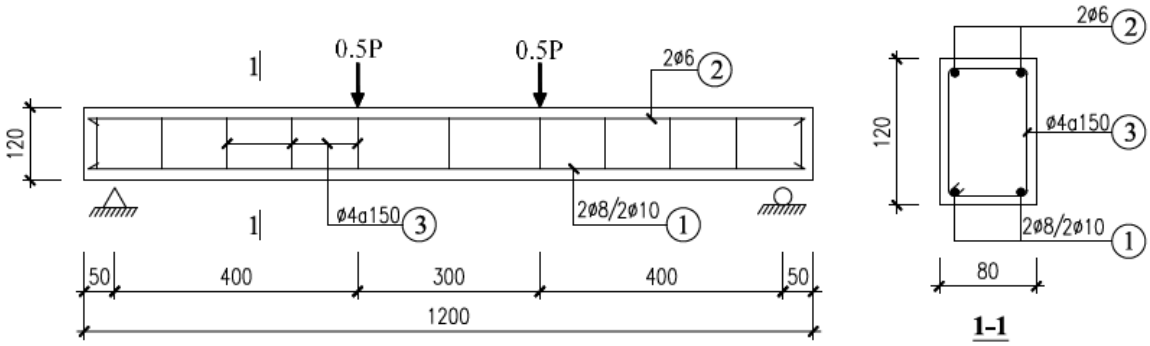

Figure 1: Schematic of the Beam Reinforcement and Support (Experimental Work) [8]

Type of steel	Area (mm^2)	Yield strength f_y (MPa)	Ultimate strength f_u (MPa)	Ultimate strain ε_{su} (%)
D6 plain bar	28.3	288.6	419.3	29.3
D8 deformed bar	50.3	334.0	437.4	25.7
D10 deformed bar	78.5	337.3	437.4	23.7

Figure 2: Steel Bars Mechanical Properties (Experimental Work) [8]

$$c\ (\%) = \frac{m_0 - m}{m_0} \times 100 = \frac{\Delta m}{m_0} \times 100$$

No	Test group	Beam	m_0 (g)	m (g)	Δm (g)	c (%)	A_s (mm^2)
1		D8-1	390.0	-	-	-	50.30
2	Group 1	D8-2	390.0	360.8	29.3	7.5%	46.53
3		D8-3	390.0	348.0	42.3	10.8%	44.88
4		D10-1	554.5	-	-	-	78.50
5	Group 2	D10-2	554.5	508.5	46.0	8.3%	71.98
6		D10-3	554.5	476.0	78.5	14.1%	67.43

Figure 3: Overall Reinforcement Corrosion Rates (Experimental Work) [8]

Geometrical idealization of the elements in the model follows the same methodology of Hassouna and Aboelezz (2025) [9], namely, for the choice of element types, meshing settings and choices of the material models. Where rebars were modeled with element type REINF264 3D line spars embedded in the meshed concrete elements, and with bilinear isotropic material model. Sheets and Plates were modeled with element type SHELL181 and with bilinear isotropic material model. Concrete and supports were modeled with element type SOLID185, supports with bilinear isotropic material model, and concrete with Druker-Prager Concrete material model combined with Hardening, Softening and Dilatation (HSD) Exponential material model. Figures {4,5,6} show the geometrical idealization, boundary conditions and meshing.

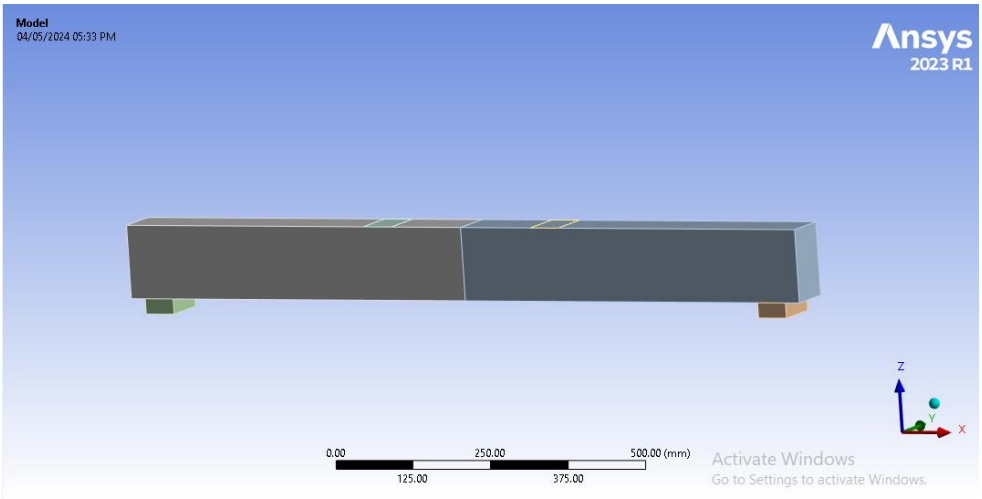

Figure 4: Full Geometrical Idealization

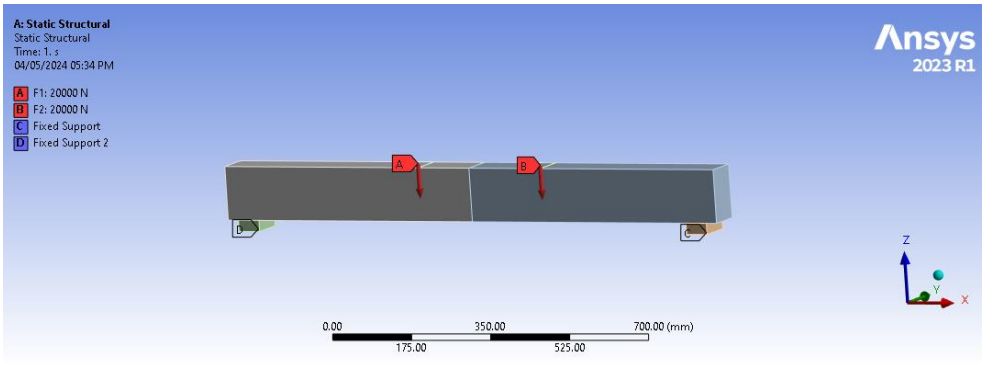

Figure 5: Boundary Conditions of the Model

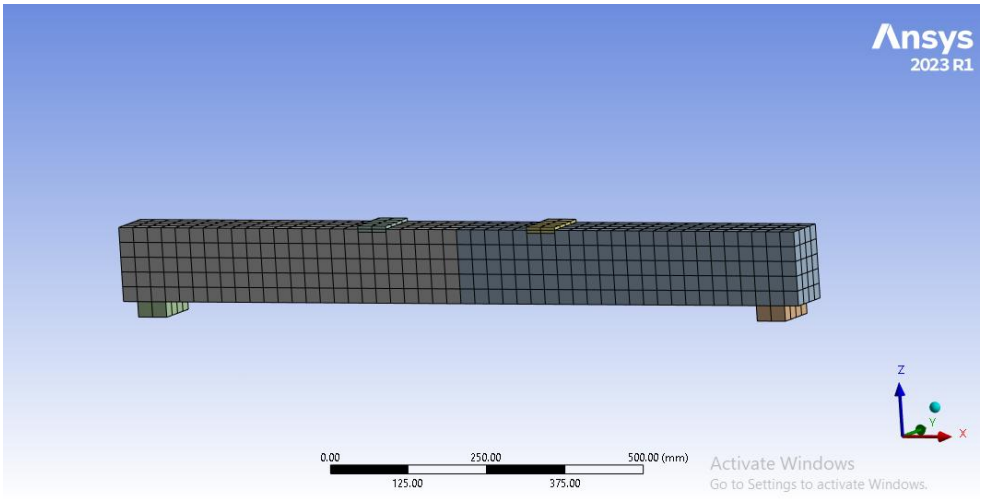

Figure 6: Meshing of the Model

As for parametric values for mechanical properties of rebars, supports and steel sheets, Poisson's ratio is taken to be 0.3, tangent modulus is taken to be 10 MPa, modulus of elasticity is taken to be 2E+5 MPa, and values of yield strength are illustrated in Table 1.

Table 1: Steel Elements Bilinear Isotropic Hardening Parameters

Element	Yield Strength (MPa)
Rebar Dia. 4 mm	240
Rebar Dia. 6 mm	285
Rebar Dia. 8 mm	335
Rebar Dia. 10 mm	335
Loading Sheets and Supports	360

As for concrete, Poisson's ratio is taken to be 0.2, estimated modulus of elasticity is taken following the expression from ECP 203 [10]

$$E_c = 4400\sqrt{f_c} \text{ in MPa}$$

Whereas the expression in ACI-318M [11] is

$$E_c = 4700\sqrt{f_c} \text{ in MPa}$$

This is to provide a slight 6.38% minimal degradation to count for any over stiffness of the initial elastic behavior compared to experiment. Hence, it is taken to be 22000 MPa.

The rest of the values of the parameters of concrete material models are illustrated in Table 2. Calculations and choices for values of uniaxial tensile strength and biaxial compressive strength is taken from common practice of 10% and 1.5 times of uniaxial compressive strength respectively. Whereas HSD parametric values follow the recommendations of Dimitriev et al. (2020) [12]

Rebars diameters were calculated based on corrosion rates and are demonstrated in Table 3.

Table 2: Parameters of Concrete within the Numerical Models

Parameter	Symbol	Values
Uniaxial compressive strength	f_c	25 MPa
Uniaxial tensile strength	f_t	2.5 MPa
Biaxial compressive strength	f_{cbi}	30 MPa
Tensile and tension-compression dilatancy	δ_t	1
Compression dilatancy	δ_c	1
Plastic strain at uniaxial compressive strength	κ_{cm}	0.012
Plastic strain at transition from power law to exponential softening	κ_{cu}	0.015
Relative stress at start of nonlinear hardening	Ω_{ci}	0.15
Residual relative stress at κ_{cu}	Ω_{cu}	0.5
Residual compressive relative strength	Ω_{cr}	0.05
Mode I area-specific fracture energy	G_{ft}	57000 N/mm
Residual tensile relative strength	Ω_{tr}	0.05

Table 3: Equivalent Diameters of Rebars in Calibration Numerical Models

No	Test Group	Beam	c%	Eq. Dia. 4 mm	Eq. Dia. 6 mm	Eq. Dia. 8 mm	Eq. Dia. 10 mm
1	Group 1	D8-1	…	4	6	8	…
2		D8-2	7.5%	3.85	5.77	7.69	…
3		D8-3	10.8%	3.78	5.67	7.56	…
1	Group 2	D10-1	…	4	6	…	10
2		D10-2	8.3%	3.83	5.74	…	9.58
3		D10-3	14.1%	3.71	5.56	…	9.27

Validation models for tests {D8-1, D8-3, D10-1, D10-3} were constructed and simulated. {D8-2, D10-2} were ignored because the experimental results showed slight increase in performance compared to control specimens. This is illustrated in Figures {7,8}.

Figures {9,10,11,12} show validation graphs between finite element models results verses experimental ones, while Table 4 shows the ultimate flexural capacities between FEA results and experimental ones, along with the deviation percentage from FEA to experimental.

FEA graphs get close to the experimental ones, with slight deviation of stiffness behavior, and where the ultimate value occurs when the solution reach a non-convergent state. Compared to the experimental ultimate values that were taken as the maximum values along the testing operation.

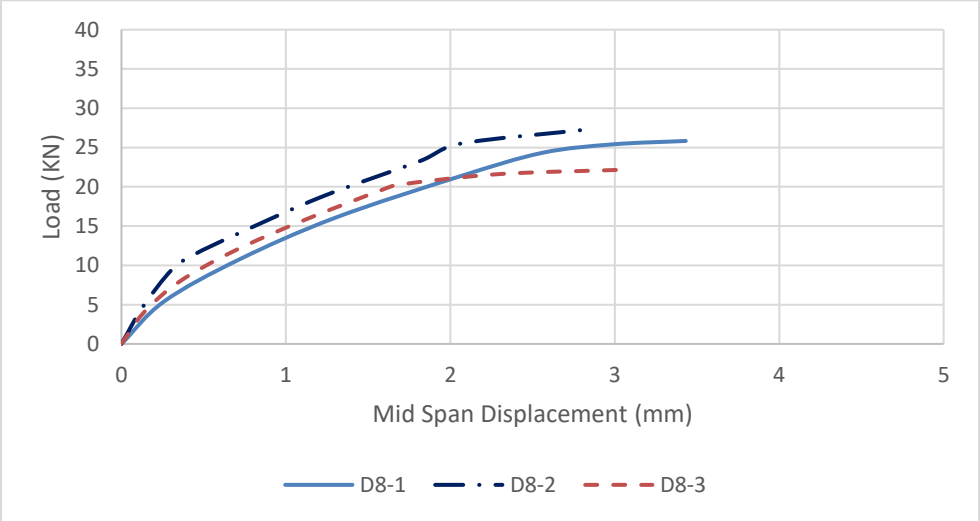

Figure 7: Load-Displacement Graphs for Testing Group of D8 (Experimental Work) [8]

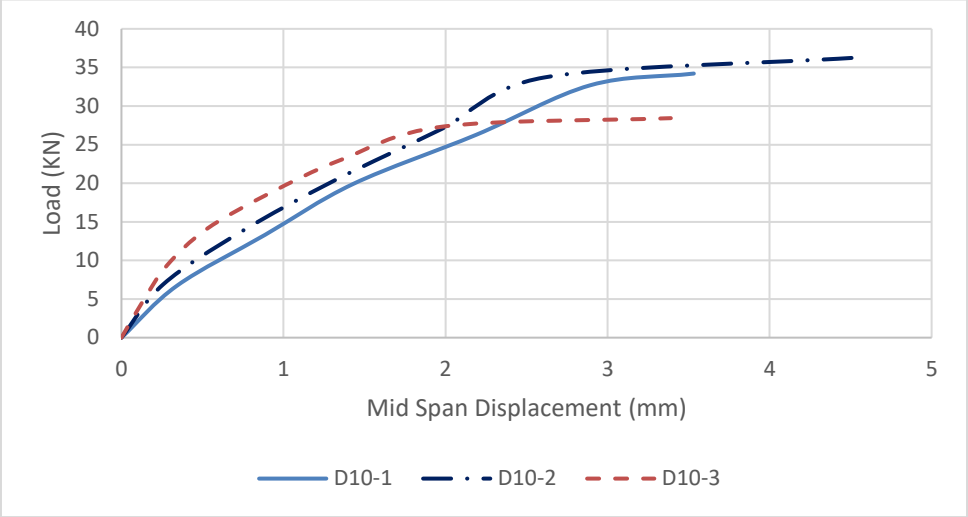

Figure 8: Load-Displacement Graphs for Testing Group of D10 (Experimental Work) [8]

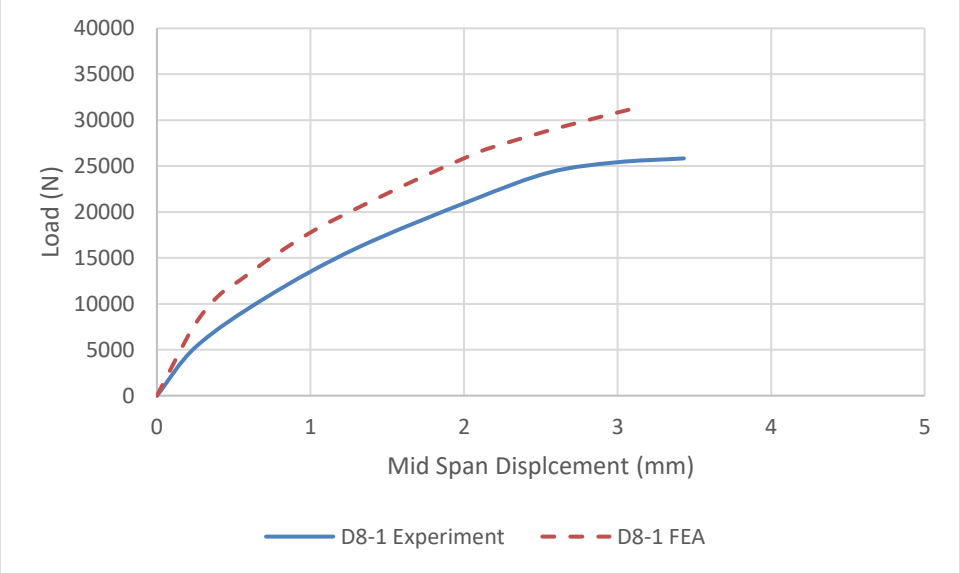

Figure 9: Load-Displacement Experiment versus Finite Element Analysis Result (Control Beam D8-1)

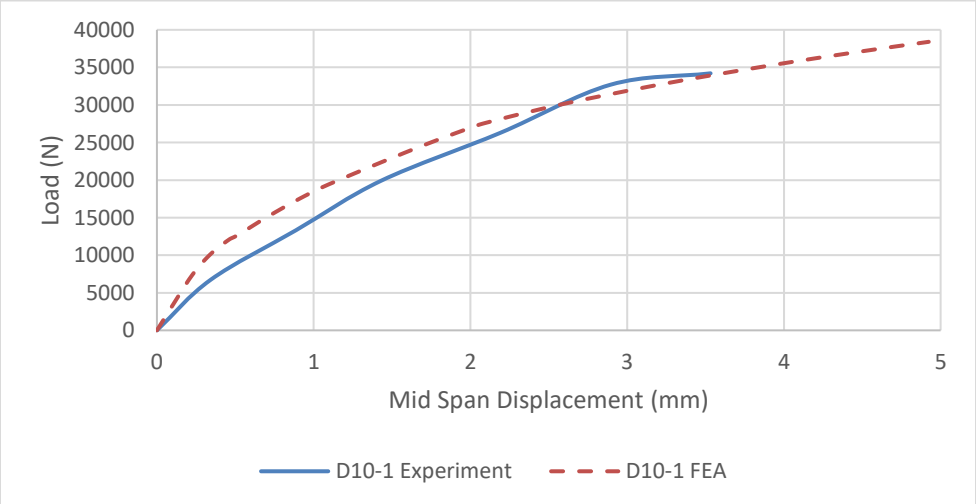

Figure 10: Load-Displacement Experiment versus Finite Element Analysis Result (Control Beam D10-1)

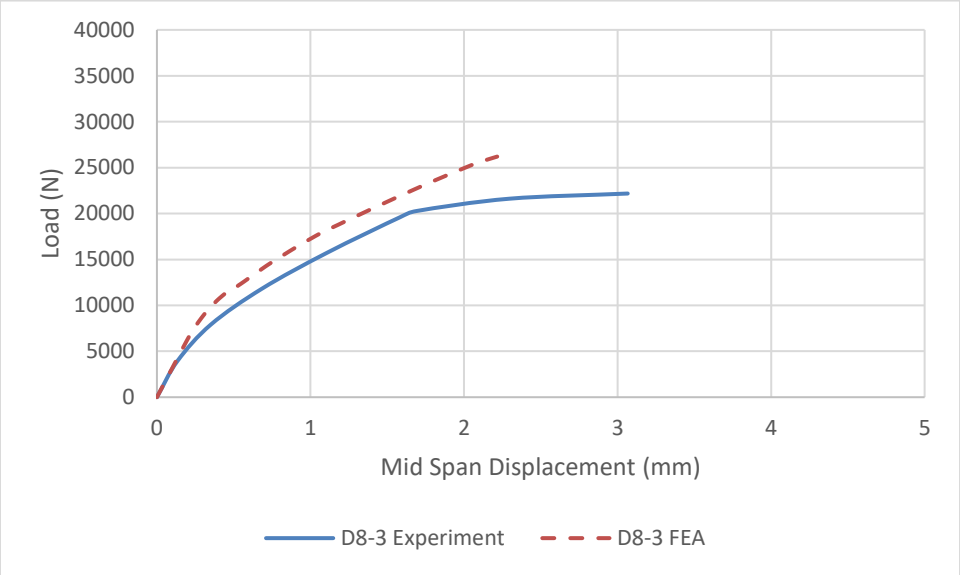

Figure 11: Load-Displacement Experiment versus Finite Element Analysis Result (Corroded Beam D8-3)

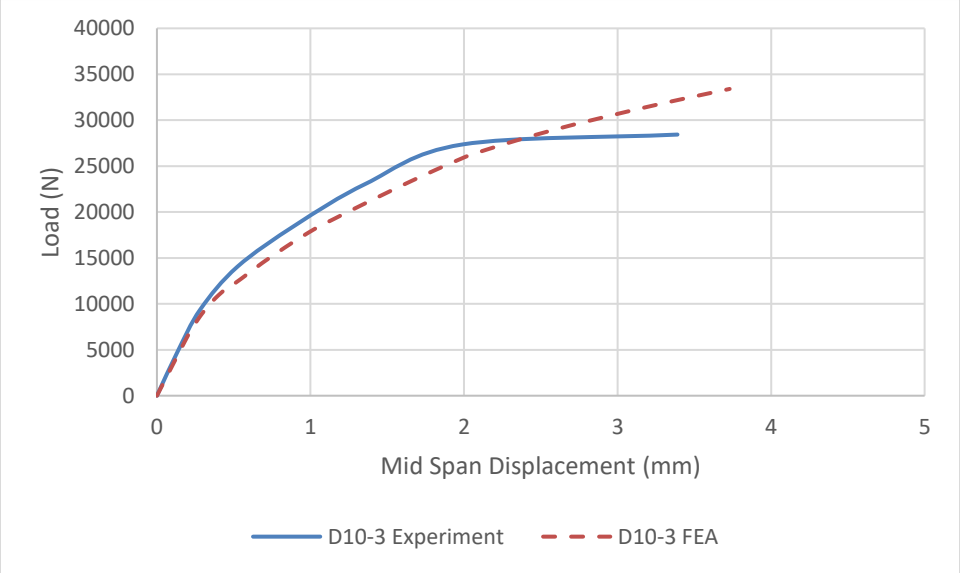

Figure 12:Load-Displacement Experiment versus Finite Element Analysis Result (Corroded Beam D10-3)

Table 4: Experimental versus Finite Element Analysis Results

Beam	Fu Experiment (N)	Fu FEA (N)	Fu_deviation%
D8-1	27406.5	31200	13.84%
D8-3	24451.5	26200	7.15%
D10-1	35768.7	38400	7.36%
D10-3	28877.1	33400	15.66%

II. DAMAGE CASE AND REPAIR FEA WORK

2.1. Damage Case, Flexural Mid Span Steel Cut

In order to demonstrate how to retrofit a damage affecting flexural capacity, and based on the previously done validation, a proof-of-concept damage case is proposed here.

With a beam of 300 mm width, 425 mm in height, and 4000 mm in span, these dimensions and the longitudinal lower reinforcement are about 3.55 times the validation model. Figure 13 shows the geometry and reinforcement of the damage case beam, figure 14 illustrates the mid-span lower rebars cut configuration showing that it is done on a 500 mm segment of the mid span, and figure 15 illustrates the load-deflection graphs with the beams with and without reinforcement cut.

In order to emulate the weak concrete behavior, uniaxial compressive and tensile strengths along with the biaxial compressive strength were set to the numerical value of the uniaxial tensile strength. Moreover, in order to decrease the stiffening behavior, uniaxial compressive strength were lowered to be 21 MPa, biaxial compressive strength to be 25.2 MPa (about 1.2 times the uniaxial compressive strength). All of that were done in order to increase the ductility behavior of the beams.

The resulted flexural capacity for the case of no reinforcement cut is 240.5 KN, and for the case of mid span reinforcement cut is 29.6 MPa.

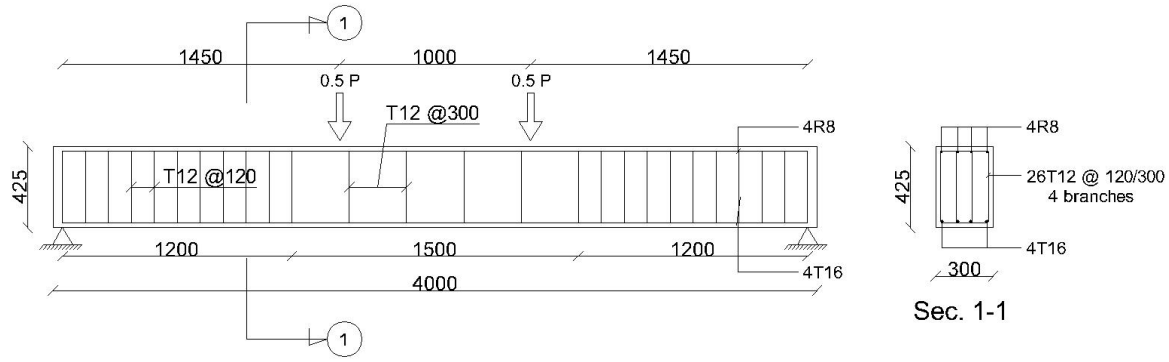

Figure 13: Geometry and Reinforcement of the Damage Case

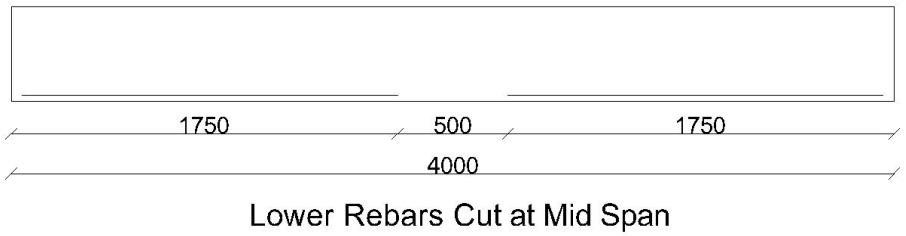

Figure 14: Lower Rebars Mid-Span Cut Configuration

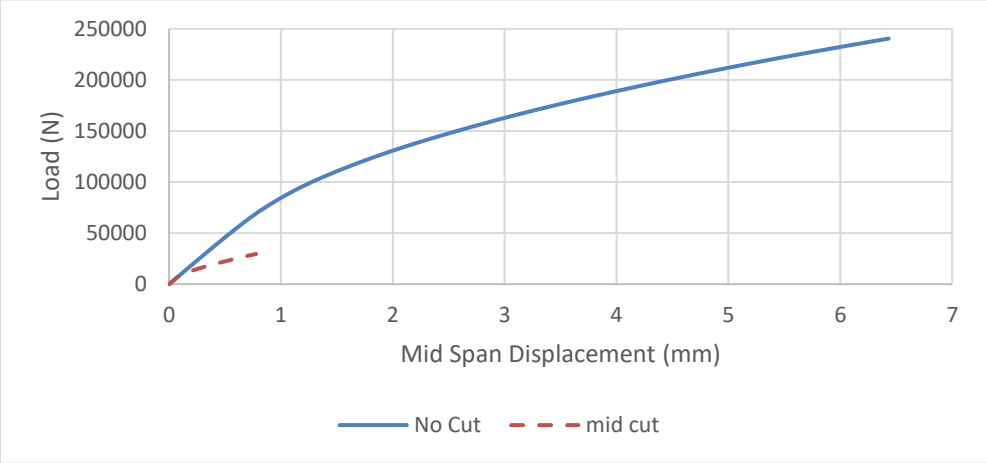

Figure 14: Load verses Mid Span Deflection of the Damage Case

2.2. Repairing with Conventional Rebars

Conventional rebars are common not only in construction but also in repairing and retrofitting techniques. Here, substitutive rebars (of the same number and diameter of the cut reinforcement) are embedded in the mid span with various cases, with no development length, with quarter the length, half the length and the full value of the development length. This is done to gauge the effect of repairing, and whether the failure can be due slipping or a predominantly due to flexural failure. Development length is calculated from ACI318 [11] to be 745 mm and is rounded to be 800 mm (rebars of 20 mm diameter were used), figure 15 demonstrates the embedment of repairing rebars with different percentages of development length, while figure 16 demonstrates the load-deflection graphs of these cases. It is worth noting that COMBIN39 elements onto the repairing rebars were applied to model the bond between them and concrete. Table 5 demonstrates the relative and restoration percentages of ultimate load capacity restoration. Relative percentage is the percentage ratio between the resulted capacity and the capacity of the beam of no reinforcement cut, while the restoration percentage is the percentage ratio between "difference between result and case of reinforcement cut" and "difference between case of no reinforcement cut and case of reinforcement cut". Figure 17 compares the least effective and best cases of rebar repairing with the damage case beams.

Figure 15: Retrofitting With Conventional Bars with Various Percentages of Development Length

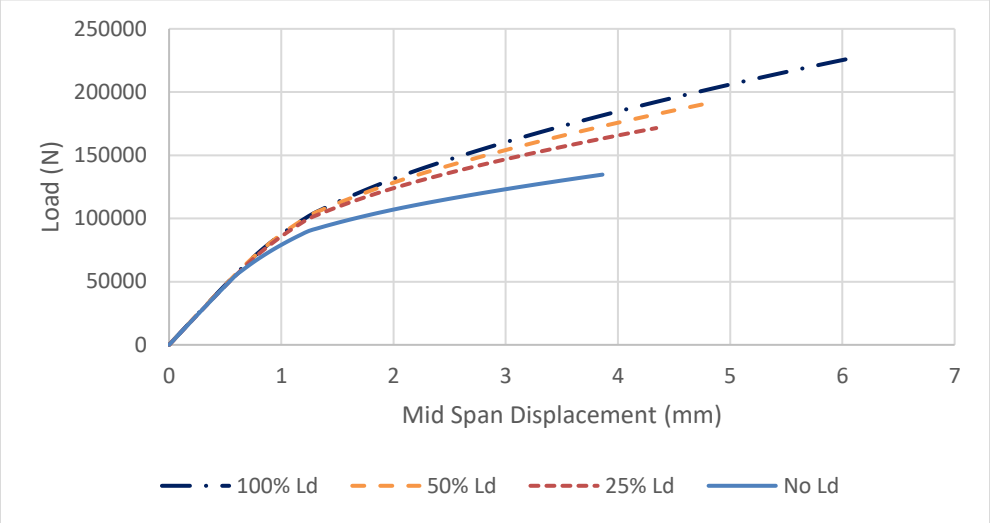

Figure 16: Load-Deflection Graphs of Beams Retrofitted With Conventional Rebars with Different Percentages of Development Length

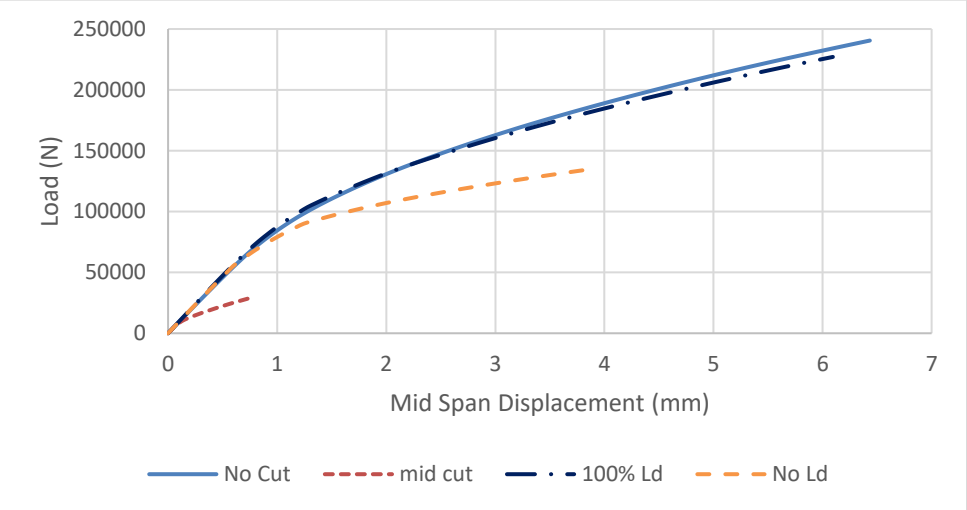

Figure 17: Load-Deflection Graphs Comparing Rebar Retrofitting with the Damage Case Beams

Table 5: Ultimate Flexural Load for Retrofitting with Conventional Rebars

Case	Fu rebars retrofitting (N)	Relative Percentage %	Restoration Percentage %
No Development Length	134671.81	60.00%	49.82%
25% Development Length	171505.41	71.31%	67.29%
50% Development Length	190904.65	79.38%	76.48%
Full Development Length	227036.53	94.40%	93.62%

When development length is implemented the results closely conform to the non-damaged case. Development length provides prolonged behavior closely identical to the original non-damaged case till a point of failure proceeding the one of the non-damaged case. This stage of "after failure" behavior is not captured in the numerical analysis as it resides within the bounds of the softening stage, at which a solution non convergence occurs, this is according to the notice of Hassouna and Aboelezz (2025) of the numerical results obtained when using Druker-

Prager Concrete material model combined with HSD material model. When development length is not implemented the plastic behavior before failure is less stiff, indicating a degree of rebars cross section decreasing due to elongation with no excess amount to count for the loss, this is occurring in the plastic stage before entering softening stage.

2.3. Repairing with Steel Plates or CFRP Sheet on the Lower Soffit

Another way of repairing is the usage of steel plates or CFRP sheet. Here, for the sake of simplicity, complete bond between the retrofitting material and concrete is assumed. The repairing material is applied only within the same span of reinforcement cut plus added fixing length to avoid debonding. Figure 111 illustrates the lengths of CFRP sheet and steel plate. CFRP mechanical properties is taken from the work of Sobuz et al. (2011) [13]. Figure 19 illustrates the CFRP mechanical properties, while the properties of steel are the same as the loading sheets and supports. The applied thickness for the CFRP sheet and the steel plates in the numerical models were calculated based on the following equation.

$$f_{y\_rebars}A_{rebars} = f_{y\_sheet}A_{sheet}$$

From this equation, CFRP thickness is calculated to be 1 mm and steel plate thickness is 4.2 mm. These values assume theoretical equivalency between the amount of reinforcement cut and the amount of the repairing replacement material. The aim for the FEA is to check if this assumed equivalency would lead to full capacity restoration, or if it would act with a degraded performance and capacity. Figure 20 shows the degraded behavior of the application of this technique, and Table 6 demonstrates the restoration percentages. Moreover, it is worth noting that covering only the span of reinforcement cut with no excess length like the usage of development length of rebars, this is due to economical purpose, as in the actual use the thicknesses are higher than the assumed numerical values, hence, the amount of used material gets higher compared to rebars.

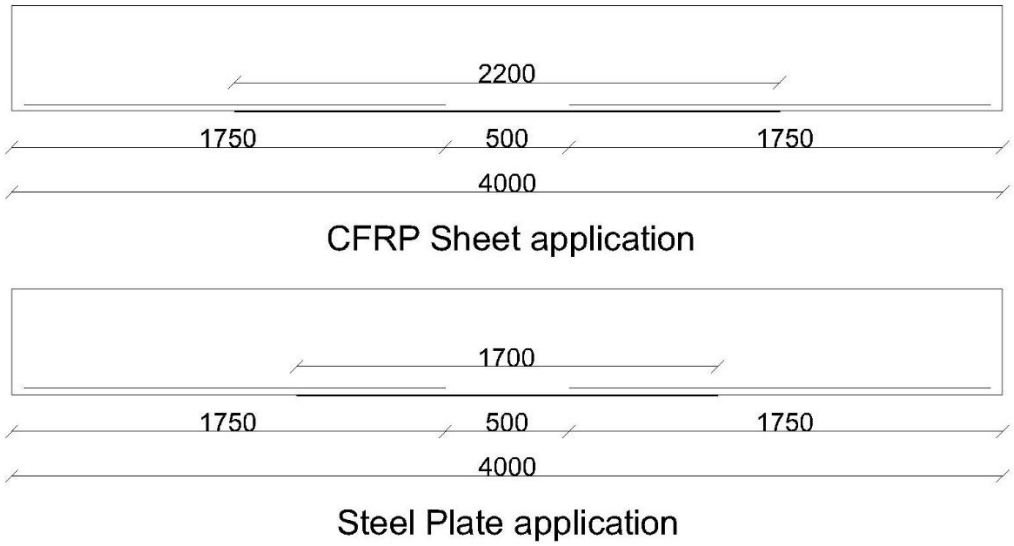

Figure 18: CFRP and Steel Plate Configuration

Materials	Property	Values
CFRP laminate	Sheet form	Uni-directional roving
	Yield strength (MPa)	1315
	Modulus of Elasticity (GPa)	165
	Elongation at ultimate (%)	2.15
	Design thickness (mm/ply)	1.2
	Tensile strength (MPa)	1685
	Density (g/cm^3)	1600
Epoxy adhesive	Modulus of Elasticity (GPa)	3
	Elongation at ultimate (%)	2.6
	Tensile strength (MPa)	55

Figure 19: CFRP Mechanical Properties [13]

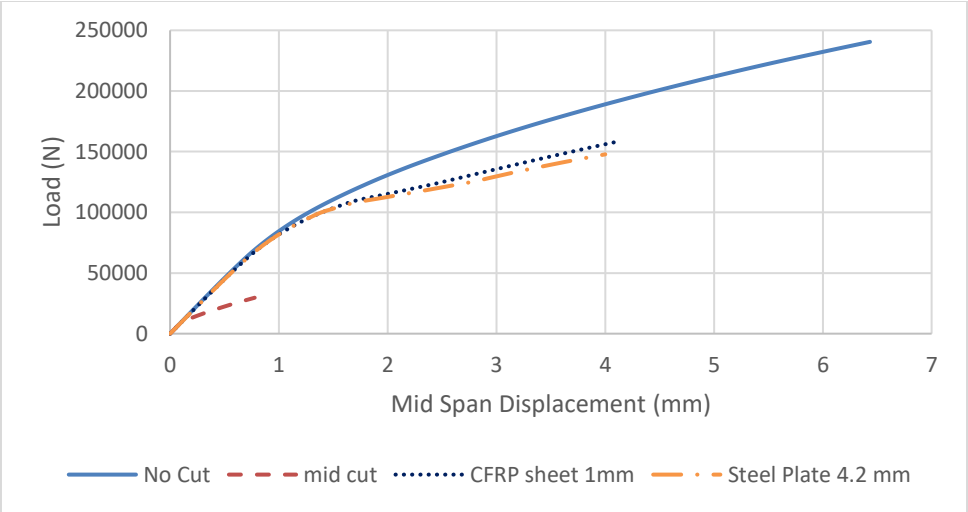

Figure 20: Load-Deflection Graphs Comparing Retrofitting using CFRP Sheet and Steel Plate on the Lower Soffit with the Damage Case Beams

Table 6: Ultimate Flexural Load for Retrofitting with CFRP Sheet and Steel Plate

Case	Fu retrofitting (N)	Relative Percentage %	Restoration Percentage %
CFRP Sheet	158063.15	65.72%	60.91%
Steel Plate	147800	61.46%	56.05%

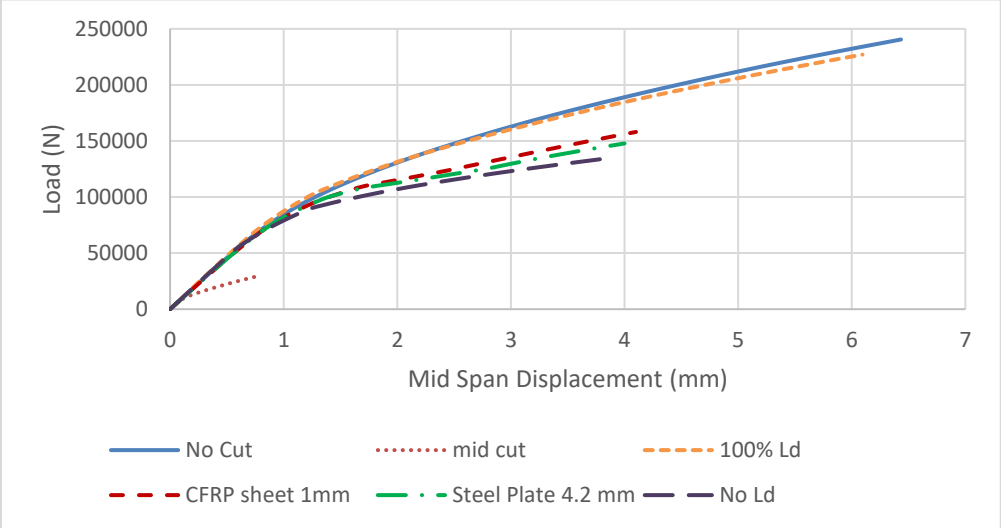

Figure 21: Load-Deflection Graphs Comparing the Second Method of Repair with Using Rebars with no Development Length

From the results illustrated in figures {20, 21} the performance degradation of using this method is closely identical to the case of using rebars with 25% development length applied. This is an indication that the behavior of the CFRP sheet and the steel plate onto the beam give less compatibility compared to using regular rebars with the highest possible development length which provides the highest possible compatibility.

III. CONCLUSION

The application of both retrofitting methods provide various effectiveness into the restoration of the ultimate capacity. Though these methods are simple and intuitive, the restoration effectiveness for the proof-of-concept case study reaches slightly near to 100% of the target capacity when using conventional bars with 100% development length, however, the use of sheets whether steel or CFRP is less effective.

The best method here is the use of rebars with the full value of development length. This method provides 93.62% of restoration, with 94.40% of the undamaged capacity, these results are for the presented proof-of-concept case study. The use of rebars with 50% development length is also feasible, providing 76.48% of restoration and 79.38% of the undamaged capacity. While the other method of the application of a retrofitting material onto the lower soffit along the span of the reinforcement cut provides poor results and degraded performance. Where the least effective case here is the use of steel plate, with 56.05% of restoration and 61.46% of the target capacity for this proof-of-concept damage case study. Moreover, CFRP sheet application has also poor performance which is slightly better than CFRP sheet, with 60.91% of restoration and 65.72% of the target capacity for this proof-of-concept case study.

REFERENCES

[1]. Siddika, A., Al Mamun, M. A., Alyousef, R., & Amran, Y. H. M. (2019). Strengthening of reinforced concrete beams by using fiber-reinforced polymer composites: A review. Journal of Building Engineering, 25, 100798

[2]. Habib, M. A., Torkey, A. A., Alnahhal, W., & Abdelrahman, A. A. (2018). Nonlinear finite element modeling of RC beams strengthened with CFRP sheets. *Engineering Structures*, 168, 523–538.

[3]. Samani, H. R. R., Lotfi-Omran, O., & Soudki, K. A. (2018). Experimental investigation of torsional strengthening of RC beams using externally bonded CFRP composites. *Construction and Building Materials*, 165, 155–167.

[4]. Mattar, I. S. A. I. (2019). Nonlinear finite element modelling for reinforced concrete beams retrofitted with FRP in bending. Physical Science International Journal, 21(4), 1-20.

[5]. Kim, M. S., & Lee, Y. H. (2021). Flexural behavior of reinforced concrete beams retrofitted with modularized steel plates. *Applied Sciences, 11*(9), 2348.

[6]. Shadmand, M., Hedayattasabdi, A., & Kohnehpooshi, O. (2020). Retrofitting of reinforced concrete beams with steel fiber reinforced composite jackets. *International Journal of Engineering, Transactions B: Applications, 33*(5), 770-783.

[7]. Ghalla, M., El-Sayed, A. A., & Sharaky, I. A. (2024). Strengthening of reinforced concrete beams with insufficient lapped splice length of reinforcing bars. Engineering Structures, 319, 118922.

[8]. Nguyen, N. T., & Nguyen, N. D. (2019). An experimental study on flexural behavior of corroded reinforced concrete beams using electrochemical accelerated corrosion method. Journal of Science and Technology in Civil Engineering, NUCE, 13(1), 1–11.

[9]. Hassouna, S. A. T., & Aboelezz, A. E. Y. (2025). Numerical calibration for torsional retrofitting of RC beams with near surface mounted (NSM) continuous spiral reinforcement. Journal of Advanced Engineering Trends, 44(1), 352–359.

[10]. Egyptian Code for Design and Construction of Concrete Structures (ECP 203-2007).

[11]. ACI Committee 318, ACI 318M-14.

[12]. 2014Dimitriev, A., et al., Calibration and Validation of the Menetrey-William Constitutive Model for Concrete. Construction of Unique Buildings and Structures, 2022. 88.
[13]. Sobuz, H. R., Ahmed, E., Hasan, N. M. S., & Uddin, M. A. (2011). Use of carbon fiber laminates for strengthening reinforced concrete beams in bending. International Journal of Civil and Structural Engineering, 2(1), 67–84.